WOOD RESEARCH
60 (3): 2015
339-350

ASSESSMENT OF WOOD SURFACE DEFECTS BASED ON 3D IMAGE ANALYSIS

Andrzej Sioma
Agh University of Science and Technology, Faculty of Mechanical Engineering and Robotics, Department of Process Control
Krakow, Poland

(Received July 2014)

ABSTRACT

This article presents the subject of analysis and the using of 3D images in a task of automatic detection and location of defects on wood surfaces. It discusses defects which occur on wood surfaces and presents examples of the most common defects recorded on production lines in the timber industry. The following section of this paper presents a method of building a 3D image of the surface using the laser triangulation method (LTM). The algorithm used to analyse the 3D image, which provides initial processing of the image in the scope of filtering and enhancing the characteristic properties of the image is discussed. Both height profile analysis and image analysis are employed in order to isolate the characteristic parameters of the defect. For selected defects, measurement algorithms which enable a parametric description of the defect and its location on the surface are presented.

KEYWORDS: Wood defects, 3D vision system, 3D image, triangulation, image analysis.

INTRODUCTION

Increasing capacity of production lines applied in the timber industry made it necessary to develop innovative solutions in the scope of systems for diagnosing and detecting wood surface defects. These solutions must be characterized by swift operation, reliability and high efficiency. Vision systems introduced into production lines enabled fast acquisition and an analysis of a image, using various methods intended to recognize and locate the defects. The vision methods usually employ an analysis of shades of grey or colours, described in studies (Hu et al. 2004, Sandak and Tanaka 2005, Nystrom and Hagm 1999, Kim and Koivo 1994). Other known solutions employ an analysis of tomographic and thermal images, discussed in the study (Wei et al. 2009, Meinlschmidt 2005). Also carried out work on the potential relationship between the tomograms and hardness maps was discussed quantitatively for improving the acoustic tomography interpretation (Lilang and Fu 2012). In many cases, in addition to defects in wood

for reasons of utility is important to assess the aesthetic surfaces such as wood grain orientation and surface color (Song and Zhao 2011).

Most vision systems can be described as 2D systems, due to information available from the image and the method of performing measurements on the image. Nowadays, industrial vision systems perform a vast array of control and measurement tasks on production lines, as part of industrial product quality control. They are usually introduced as additional equipment for technological machines and production stations. One can also observe production lines being fitted with autonomous and advanced vision stations, tasked with inter-operational control of product parameters. The introduction of automatic vision stations is particularly visible in serial production, which requires the inspection of all the products in the "0 discard" system, repetitive and fast performance of control procedures. This study presents a new approach enabling the application of a 3D vision system in the tasks of inspecting selected parameters of the product, together with the methodology of its use in order to recognize wood defects. One advantage of this method is that the range image allows us to perform much more measurements and tests, particularly in the scope of spatial measurements, supplementing and expanding the applied inspection methods (Michalec et al. 2011, Kowal et al. 2012). Yet, due to the method of constructing 3D images using the laser triangulation method (LTM), a more detailed analysis of the interaction between the laser and the surface inspected in the function of the adopted vision system setup is required. Due to the fact that vision systems are setup and constructed strictly with a view to complete diagnostic tasks, further works related to the construction of a vision system and the preparation of diagnostic software which employs the developed methodology must be preceded by a detailed task analysis and tests carried out both in the laboratory and on the production line. The visual system presented in this study was designed and launched in the Production Process Automation Laboratory of AHG University of Science and Technology, and, after laboratory tests, it was tested industrially, in quality control tasks for the surface quality of parquet blocks and planks.

Wood defects visible on its surface decrease product value, and in many cases can even cause their rejection as material for a particular purpose. They are described in standards, but their parameters are frequently specified much stricter in the order documentation issued by manufacturers who use the wood as material. Therefore, the designed visual system should feature a setting for values of parameters which define these defects. The most common defects include: Knots, eccentric pithing, double pithing, cracks and defects caused by rot or fungi.

Knots significantly decrease the technical properties of timber. From the perspective of mechanics, knots are hard, local intrusions which disturb the homogeneity of wood and the straight direction of the grain. The knots adjoin concentrations of stresses and discontinuities of material. As a result, the knots significantly decrease the tensile and bending strength of the wood and, to a lesser extent, its compression strength. The figures below present a product in the form of a glued board made of material which contains various types of knots (Fig. 1).

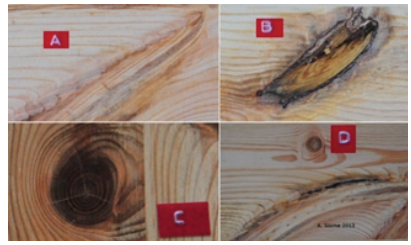

Fig. 1: Examples of different knots on wood surfaces.

The above drawing presents four examples of knot images:
A - half leaf, healthy, light knot,
B - elongated knot, rotten knot, the wood around the knot contains resin,
C - knots round, healthy and dark knots,
D - winged-sided, partially fused, spoiled.

The objective of the research was to develop a vision system that uses a MTL method for constructing the range image of the wood surface. This image should contain information about the defects present on the surface of the wood. The algorithm developed for image analysis is used for location, description and evaluation of the parameters of knots on the wood surface in industrial environment.

MATERIAL AND METHODS

The construction of a 3D vision system requires the system setup to be chosen appropriately to the task at hand (Kowal and Sioma 2009, 2010, 2012). It is necessary to select the parameters of all the devices which form the system. Among these, particular attention should be paid to the parameters of the mutual arrangement of the camera and laser illumination, the visual system matrix resolution, parameters of the optical system, and parameters of the laser illuminator. The system geometry is defined as the spatial interrelation of the camera, laser illumination and the object inspected. Specification of the geometry allows us to determine the resolution of the constructed 3D image. The position of the surfaces which form the object inspected in relation to the vision system is also of great importance for the quality of the 3D image. When preparing the geometry of the 3D vision system, the following parameters should be taken into consideration: The dimensions of the investigated object, possibility of enclosing the vision system, the field of view and the set of object properties subject to assessment.

The construction of a 3D image is made on the basis of analysing a 2D image captured by the camera which observes the laser line traced on the surface (Fig. 2a). Then, the laser triangulation method (LTM) is applied to determine the heights of all the points which make up the height profile (Fig. 2b) along the laser line. Joining a group of profiles allows us to construct a 3D surface image.

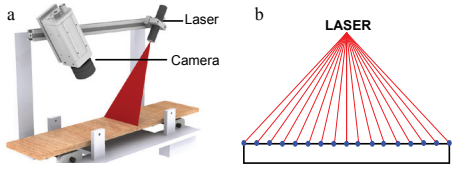

Fig. 2: Object illumination a) and the arrangement of measuring points for 3D VS setup b).

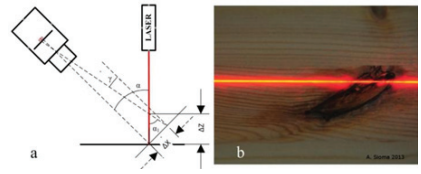

Fig. 3: Setup of the vision system a) and image of the line projected onto the wood surface for B-type knot b).

The wood defects are measured using the geometry of the 3D vision system shown in Fig. 3a, where the sensor of the vision system is situated at an angle of 90-α relative to the measuring table surface. The laser plane is perpendicular to the inspected surface and set at angle α relative to the optical axis of the camera (Fig. 3a).

The height profile determined on the basis of analysing the laser line image corresponds to the cross profile. This profile is observed by the vision system set at 90-angle (Fig. 3a). Consequently, it is necessary to convert the geometry of the section visible to the camera in order to obtain the actual cross-section. Each profile determined on the examined surface is described with a one-dimensional matrix (Fig. 3b). It contains a set of values which define the height for the measuring points determined along the laser line visible on the examined surface. The points which define the height profile are outlined with resolution depending on the adopted setup, the applied optical system and the resolution of the vision system sensor. As a result of the changed height of the object illuminated with the laser line, the image of this line moves on the vision system sensor (Fig. 3a). The determination of the 3D vision system resolution consists in the determination of three component resolutions for each axis of the coordinate system. For axis Z, this consist in the determination of a minimal change to the object height, defined by parameter ΔZ, at which it is possible to observe the laser line move by precisely one row of the pixels on the sensor (Fig. 3a). On a plane parallel to the sensor surface, a resolution ΔX was determined along the X axis, on the basis of the field of view (FOV) dimensions, and the resolution of the sensor specified in the pixels. The ΔY resolution along the Y axis is defined as the distance between the acquisition of the subsequent height profile images for the investigated object. Assuming the application of a sensor sized 1536x512 pixels and choosing the lens of the vision system which enables the observation of an object 128 mm wide (FOV = 128 mm), resolution along the X and Y axis was determined for the configuration applied.

$$\Delta X = 128 \text{ mm} / 1280 \text{ pixels} = 0.1 \quad \text{(mm/pixel)} \tag{1}$$

When calculating the resolution along the Z axis of the station, an approximation assuming that the α angle is equal to the α_1 angle was applied. In fact, angle α_1 is equal to $\alpha - \gamma$. Applying this simplification, the resolution along the Z axis of the station is determined, accepting the angle $\alpha = 45°$.

$$\Delta Z = \Delta X/\sin(\alpha) = 0.1 / \sin(45°) = 0.07 \quad \text{(mm/pixel)} \tag{2}$$

where: ΔZ – resolution along axis Z,
ΔX – resolution along axis X,
α – angle between the optical axis of the laser and the optical axis of the camera.

The resolution along the Y axis of the coordinate system depends on the shift of the investigated surface between the subsequent image acquisitions performed by the vision system. The construction of a 3D image surface requires the determination of a height profile at subsequent positions of the object, which is moved relative to the fixed system consisting of the camera and the laser. The distance between subsequent profiles is assumed to be the resolution along the Y axis of the station. Assuming that the object movement measurement system includes an encoder which emits 1600 pulses per 1 mm of the table movement. For an image acquired every 160 pulses, the resolution along the Y axis is:

$$\Delta Y = 160 \text{ (imp/scan)} / 1600 \text{ (imp/mm)} = 0.1 \quad \text{(mm/scan)} \tag{3}$$

A 3D image constructed using the 3D vision system is defined with a square matrix (*i, j*). The *j* dimension corresponds to the x coordinate in the image coordinate system and defines the width of the vision system FOV, specifying the number of columns in the matrix. The *i* dimension corresponds to the *y* coordinate in the image-related coordinate system and defines the number of height profiles determined for the investigated object, determining the number of the matrix rows. Individual entries of the matrix present information on the image height h_x for each of the points which identify the surface.

Fig. 4 presents an image of timber with laser line projected onto the surface, as well as the line image recorded by the vision system (Fig. 4b). Construction of the range image requires the precise location of position of the laser line visible on the image. Position of the line is determined on the basis of intensity analysis in each column of the image (Fig. 4c). It should be noted that the cross section of the laser line is the set of pixels forming the intensity profile (Fig. 4a). For this profile the threshold intensity is defined for shut-off background. Then, for the intensity profile above the threshold the position of the center of gravity (COG) is determined with subpixel resolution. Location of this COG describes the position of the laser line.

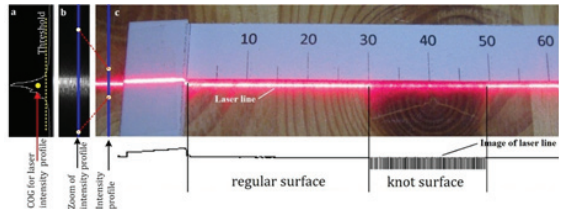

Fig. 4: High profile of timber surface with visible knots illuminated with a laser line for the C-type knot.

A new approach applied in this study is the selection of the laser output and exposure time in such a way, that the surface image would present a distinct difference between the surface of the knots and the proper wood surface. These parameters are crucial for the quality of the final 3D image and should be selected appropriately for the material. The way in which the laser light is reflected or dispersed on the wood surface directly influences proper recognition of the laser line position, and consequently the determination of the height of the points which form the height profile. The power of the laser is selected based on a series of tests, which involve the determination of the standard deviation for each of the profile points. For the chosen setup of the vision system and for the object tested, in this case the selected kind of timber, the points which form the profile for the same location of the laser line on the surface were determined n-times. This measurement allowed us to estimate the value of the standard deviation of the height measurement for the selected system operation parameters, as per the following formula:

$$\sigma(p) = \sqrt{\frac{1}{n-1}\sum_{i=1}^{n}(z_i - \bar{z})^2} \tag{4}$$

where: σ(p)– standard deviation for point "p" of the profile,
z_i – profile height value for point "p" in i-th measurement,{},
z – average height value at point "p",
n – number of measurements made for a single profile.

The value of the standard deviation was calculated for each point of the profile. This allows us to create a chart of standard deviation values for each profile point, enabling the assessment

of the way the laser light interacts with various structures present on the wood surface (Fig. 5 below). From the perspective of the potential detection of defects, the most interesting are the differences between the standard deviation for measuring the height of the points observed on the proper wood surface and on the damaged surfaces, e.g. knots. The standard deviation chart should be made for various outputs of the laser and the results should be compared for the purpose of choosing settings for the vision system. The tests were conducted using a laser which emits light with a wavelength of 658 ± 15 nm i and power output of 35 mW. In the figure below, the laser power is specified in percentage of Max Laser Power - e.g. 20 % LP. The standard deviation chart is used to locate the wood surface defects based on the assessment of the height profile.

A range image of an object contains noise and distortions arising from the method used. Minor changes in the image points height resulting from the operation of the laser light on the surface are used to determine the edge of the knots on the wood surface. The raw image of edge was subjected to smoothing, and filtering with a median filter. In both cases, a mask in the form of a 3x3 was used. Smooth filter converts the value of the central element into an arithmetic average value calculated from the eight elements that surround it. Median filter converts the value of the central element of the mask into a median value determined from the eight elements surrounding it. To strengthen edges, the Erode or Dilate filter can also be used as it enables conversion of the central element of the mask into the lowest or highest point of the eight surrounding it.

RESULTS AND DISCUSSION

Analysing the courses of the standard deviation for the heights of the points which form the height profile, one should choose such a setting of the laser power which provides the greatest visible difference between the fragment which defines the proper timber surface and the surface of knots (Fig. 5).

Another parameter important for the construction of the wood surface image is the selection of the frequency of acquiring height profiles from the surface. This frequency is related to the speed of the moving the investigated surface relative to the 3D vision system and the resolution determined for the Y axis of the 3D vision system. The tests demonstrated that for each material it is necessary to conduct a series of tests and to choose such a frequency of the vision system and laser power which would provide a surface image presenting the greatest differences between the proper surface and the knot surface (Fig. 6).

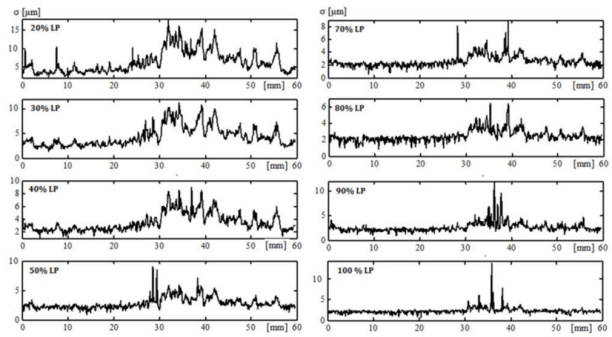

Fig. 5: Standard deviation chart determined for 600 points forming the height profile for the selected location of the laser line on the wood surface with the C-type knot.

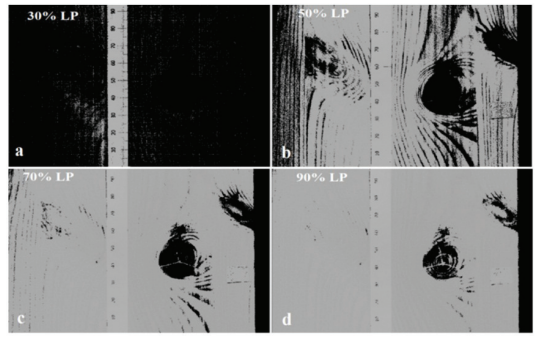

Fig. 6: The wood surface image recorded using various laser power for the C-type knot; a) 30 % of laser power (LP=35 mW), b) 50 % of laser power, c) 70 % of laser power, d) 90 % of laser power.

The 3D surface images shown in Fig. 6 are presented as a projection on the XY surface. They present four different 3D images of the same surface. The images were made at a frequency of 1500 profile/s and for four values of power. Assessing the results, it can be concluded that the task of locating the knots on the wood should be carried out with this frequency for powers above 70 % LP. Images 6c and 6d include areas which explicitly define the location of the knot. Image 6b includes additional information about the layout of the rings around the knot, which also can be used for the assessment of the material. Whereas the images made with laser power below 50 % LP are unsuitable for the location of defects.

The analysis of the 3D images is based on the processing of data specifying the height of points which form the surface, collected in a 2D matrix. Such an image may be scaled from the value of the pixels defined by the height of the consecutive surface points which form the 3D image into values expressed in shaded grey and is applied as an auxiliary method, particularly in surface visualization operations.

This study provides a discussion of an algorithm which enables the processing of 3D (range) images, based on an analysis of the data collected in the image, in the form of the height of each pixel forming the image. The purpose of such an analysis is to determine the characteristic properties of the image and to present them in the form of parameters. Usually, such parameters are: the geometric dimensions, the surface areas, the volume, or the shape of the defects defined in a defect catalogue. An analysis of a 3D wood surface image can be divided into three stages: Preprocessing, measurements of select parameters, and the assessment of the measurement results.

Recorded 3D images are subject to pre-processing in order to remove interference and to refine those properties of the image which are employed at the stage of measuring the characteristic parameters. The pre-processing is performed using point, contextual and morphological transformations. Point transformations of an image are carried out point by point, using the height value of each point. These include thresholding or scaling of the image. Contextual transformation of a 3D image enables transforming the height value of each pixel, yet taking into account the value of the points situated around it. An example is a filter allowing us to supplement the data for the pixels which, due to the interference, had no height determined. The pre-processing stage includes also morphological transformations which, for instance, allow us to refine such properties of the image as edge visibility, and smoothing of the edges and surfaces.

The surface image of an A-type knot, presented in Fig. 7a, was obtained through an analysis of the edges visible in a 3D image. The purpose was to determine the disturbances in the layout

of rings around the knot relative to their arrangement on the proper wood surface. Based on an analysis of the ring layout in a reference area, the direction of the edge analysis was selected and disturbances present on the surface were determined.

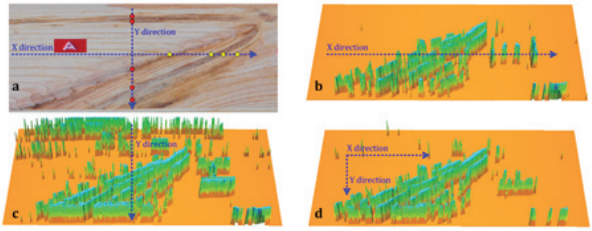

Fig. 7: The 3D image of the wood surface: a) – the image of the knot-A, b) – the edge image searched along the X axis, c) – edge image searched along the Y axis, d) – edge image sought, taking into account the neighborhood of points in the direction of X and Y.

An edge analysis allows us to select the parameters of their determination and, as a result, allows us to build various end images. The parameters include: The height and width of the edges in question, the number and order of the transformations related to the filtration of the 3D image, as well as the direction of the edge tracking. Now it should be emphasized that these parameters must be selected based on a test carried out in an industrial environment. This experiment allows us to recognize all disturbances which may appear on the examined wood surface. Next, these tests should serve as the grounds for selecting the system parameters for each type of wood.

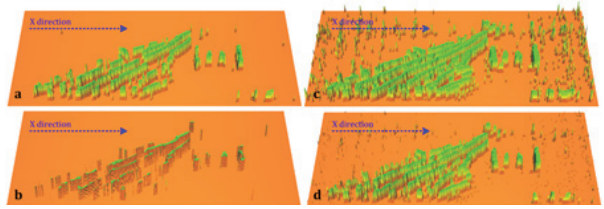

Fig. 8: The 3D knot image for 4 examples of parameter sets applied at the stage of pre-processing a 3D image.

The image shown in Fig. 8b allows us to assess the characteristic properties of knot edges, whereas the image shown in Fig. 8a enables a better assessment of the area occupied by the knot. Disturbances are visible in Figs. 8c and 8d, and they result from the type of filtration applied during the construction of the end surface image. The table below presents the transformation used in the image analysis of the knot type A. Edge image determined in the direction of axis X was used (Fig. 7b). The parameter E_p = 0.07 define the minimum edge height visible as edges on the surface. Next parameter in table indicates the order and type of used filters.

Tab. 1: Parameters of the construction the 3D images visible in Fig. 8.

Figure	Suorce	Edge par.	1st filter	2nd filter	3rd filter
Fig. 8a	Raw 3D image	Ep =0.07 mm X -direction	Median M 3x3	Smoth M 3x3	Dialate M 3x3
Fig. 8b	Raw 3D image	Ep =0.07 mm X -direction	Median M 3x3	Smoth M 3x3	Erode M 3x3
Fig. 8c	Raw 3D image	Ep =0.04 mm X -direction	Median M 3x3	Smoth M 3x3	Dialate M 3x3
Fig. 8d	Raw 3D image	Ep =0.04 mm X -direction	Median M 3x3	Smoth M 3x3	Erode M 3x3

An analysis of the defect parameters was also supported by tests related to the construction of a 3D surface image using auxiliary plane. A series of tests related to the selection of the parameters for this transformation was carried out, and the results are presented in the figure below. It shows images acquired by the visual system and the end images obtained by transformations for two sets of parameters. The raw surface image for the first set is visible in Fig. 9a and after the transformation in Fig. 9b. Identically, for the 3D image shown in Fig. 9c, the post-transformation image is presented in Fig. 9d. The rings visible on the proper wood surface in both cases are arranged in parallel to the edge of the reference rule visible in the middle section of the 3D surface image. Apart from the knot area, the image shown in

Fig. 9b presents an excessive quantity of details which hinder both the analysis of the knot location and the calculation of its surface area. The image shown in Fig. 9d presents the knot surface in a precise manner, enabling the assessment of its dimensions and location. Parameters of the image construction shown in Fig. 9a are described in Fig. 6b, parameter of the image construction shown in Fig. 9c are described in Fig. 6d.

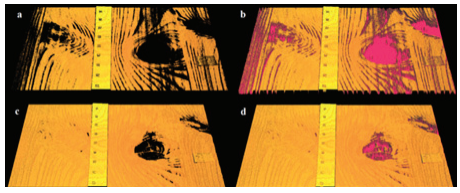

Fig. 9: A comparison between 3D images for two set of parameters a–b and c–d.

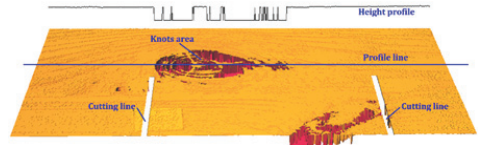

Fig. 10: Location of the knot using height profile analysis.

The first stage of a 3D image analysis is carried out in order to prepare an image of a defect, e.g. a knot, for the measurement task. The measurement task will include the determination of the parameters which define the defects. They can be, for instance, dimensions of a defect, its surface, or coordinates which specify the location of the knot on the products.

Measurements describing the defect parameters were also made for the knot image shown in Fig. 1c and its 3D image presented in Fig. 9d. The image prepared in the pre-processing stage was used to determine the edges specifying the location of the defect. The edges were determined through an analysis of the surface height profile determined on the basis of a surface analysis conducted along the line shown in the image below (Fig. 10). The determination of their location allows us to determine the boundaries of the area occupied by the knot. This analysis is used to define the line of cut which is required to remove the determined defect from the material.

Additionally, a set of parameters required for a parametric description of the defect can be determined on the 3D image (Fig. 11). These can include: The location of the defect centre, the width and length of a rectangle circumscribed on the defect, parameters describing the shape, e.g. ovality and perimeter. The determined values enable a parametric description of each defect and they were used to define the location of the line along which the height profile was determined.

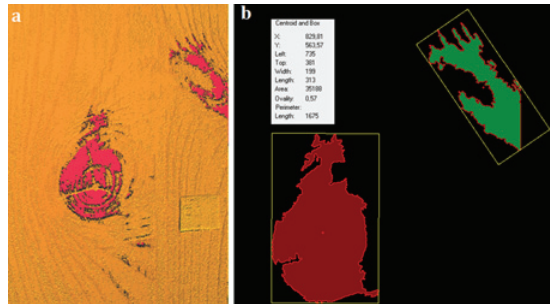

Fig. 11: Location of the knot using area of knots analysis on the 3D image.

The defect is assessed and classified on the basis of the determined parameters. The defects are classified based on the assumed parameters which define their acceptable dimensions, prepared by the process engineer. The selected parameters which describe the knots, e.g. centre location and the dimensions of the knot area are transferred to the PLC operating in the machine control system (Dominik 2009). This controller performs the procedure of removing or marking of the defects, using actuation systems installed at the product control station.

CONCLUSIONS

The application of 3D image analysis in the scope of finding, locating and assessing wood surface defects in the form of knots is a new technology intended for implementation in production lines. The innovative method of choosing set points for the 3D vision system presented herein allows us to build wood surface images which precisely define the defect areas. One should notice very distinct differences between the areas specified as defects and areas considered proper surfaces visible in 3D images. An analysis of the defective areas enables precise and repeatable descriptions of the defect parameters and their classification. This allows for fast sorting of material on a production line.

An analysis of a 3D wood surface image can be presented in the form of an algorithm, a diagram of which is shown in Fig. 12. The 3D image is constructed using the vision system, and then preprocessed in order to prepare it for measurement procedures. The next steps are: measurements of key parameters, classification of defects and the transfer of data to the production control systems. The data are also transferred to database systems enabling the assessment of the production process.

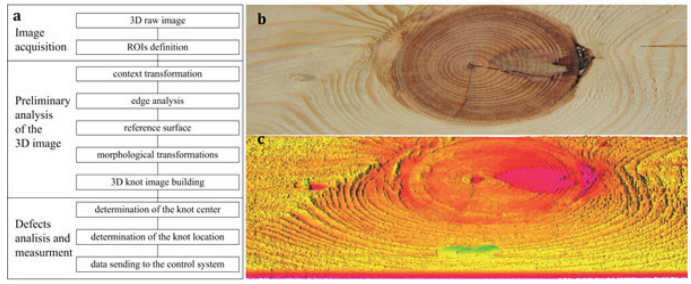

Fig. 12: Schematic diagram of the reconstruction algorithm (a), b – image of the wood surface, c – 3D image of surface with the knot.

The developed method of assessing timber defects based on an analysis of 3D images allows us to perform much more measurements and tests, particularly in the scope of spatial measurements. This significantly expands the capacity for the proper assessment of surface defects, compared to an analysis using vision systems which apply an analysis of images containing information about the shades of grey or the colour of the investigated surface.

ACKNOWLEDGMENTS

This paper was written as part of statutory research carried out at the AGH University of Science and Technology, Faculty of Mechanical Engineering and Robotics, Department of Process Control.

REFERENCES

1. Dominik, I., 2009: Implementation of the type-2 fuzzy controller in PLC. Diffusion and Defect Data – Solid State Data. Pt. B, Solid State Phenomena; 2010, 164: 95-98, ISSN 1012-0394
2. Hu, Ch., Tanaka, C., Ohtani, T., 2004: Locating and identifying sound knots and dead knots on sugi by the rulebased color vision system. J. Wood Sci. 50(2): 115-122.
3. Kim, C.W., Koivo, A.J., 1994: Hierarchical classification of surface defects on dusty wood boards. Pattern Recognition Letters 15(7): 713-721.
4. Kowal, J., Karwat, B., Sioma, A., 2012: Using three-dimensional images in the description of environment and biological structures. Polish Journal of Environmental Studies 21(5A): 227-232.
5. Kowal, J., Sioma, A., 2009: Active vision system for 3D product inspection. Learn how to construct three-dimensional vision applications by reviewing the measurements procedures. Control Engineering USA 56(11): 46-48.
6. Kowal, J., Sioma, A., 2010: The method of building 3D product image using vision system. (Metoda budowy obrazu 3D produktu z wykorzystaniem systemu wizyjnego). Acta Mechanica et Automatica 4(1): 48-51, ISSN 1898-4088 (in Polish).
7. Kowal, J., Sioma, A., 2012: Surface defects detection using a 3D vision system. In: 13th International Carpathian Control Conference (ICCC). Pp 382-387.

8. Lilang, S., Fu, F., 2012: Relationship analysis between tomograms and hardness maps in determining internal defects in Euphrates poplar. Wood Research 57(2): 221-230.
9. Meinlschmidt, P., 2005: Thermographic detection of defects in wood and wood-based materials. In: 14th (May 2nd-4th 2005) International symposium of nondestructive testing of wood, Hannover, Germany. Pp 39-46.
10. Michalec, K., Wąsik, R., Barszcz, A., 2011: The effect of mechanical damage to the stems of standing spruce trees on the quality and value of their timber. Technology and Ergonomics in the Service of Modern Forestry, (Technika i ergonomia w służbie współczesnego leśnictwa. Wydawnictwo UR w Krakowie), monograph. Pp 503-513 (in Polish).
11. Nyström, J., Hagm, O., 1999: Real-time spectral classification of compression wood in *Picea abies*. J. Wood Sci. 45(1): 30-37.
12. Sandak, J., Tanaka, C., 2005: Evaluation of surface smoothness using a light-sectioning shadow scanner. J. Wood Sci. 51(3): 270-273.
13. Song, S.S., Zhao, G., 2011: Psychological and emotional reactions to anatomical patterns in wood. Wood Research 56(4): 455-466.
14. Wei, Q., Chui, Y.H., Leblon, B., Zhang, S.Y., 2009: Identification of selected internal wood characteristics in computed tomography images of black spruce: A comparison study. J. Wood Sci. 55(3): 175-180.

Andrzej Sioma
AGH University of Science and Technology
Faculty of Mechanical Engineering and Robotics
Department of Process Control
Al. Mickiewicza 30
30-059 Krakow
Poland
Phone: +48 12 617 5005
Corresponding author: andrzej.sioma@agh.edu.pl